Electronic Supplementary Material (ESI) for Polymer Chemistry.

Electronic Supplementary Information for:

The Effect of Polarity on the Molecular Exchange Dynamics in Imine-based Covalent Adaptable Networks

Sybren K. Schoustra,[a] Timo Groeneveld,[a] Maarten M. J. Smulders*[a]

[a] Laboratory of Organic Chemistry, Wageningen University, Stippeneng 4, 6708 WE Wageningen, The Netherlands.

* Corresponding author: maarten.smulders@wur.nl

Table of Contents

1. General

All solvents (tetrahydrofuran, dichloromethane, dimethylformamide, ethanol, ethyl acetate, heptane and $CDCl_3$) were bought from either Sigma-Aldrich, Tokyo Chemical Industry (TCI) or Alfa Aeser. Terephthalaldehyde (**TA**, 99%), benzaldehyde (99.5%), benzylamine (**BA**, 99%) and 1,8-dibromooctane (98%) were bought from Sigma-Aldrich. Tris(2-aminoethyl)amine (**TREN**, 97%) was bought from Acros Organics. Triglycol dichloride (97%) was bought from Fisher Scientific. 1,8-Diaminooctane (**DA-C**, 98%), 1,2-bis(2-aminoethoxy)ethane (**DI-O**, 98%), *p*-tolualdehyde (98%) and 4-hydroxybenzaldehyde (98%) were bought from Tokyo Chemical Industry (TCI). All chemicals were used as received unless indicated differently.

NMR spectra were recorded on a Bruker Avance III 400 MHz instrument and analysed with MestreNova software. Chemical shifts are reported in parts per million (ppm), calibrated on the residual peak of the solvent, whose values are referred to tetramethylsilane (TMS, δ_{TMS} = 0 ppm), as the internal standard. IR analyses were performed on a Bruker Tensor 27 spectrometer with platinum ATR accessory. Rheological measurements were conducted on an MCR 501 Anton Paar rheometer in combination with a temperature-controlled plate-plate configuration and temperature controller hood for additional thermal homogeneity.

2. Small-molecule kinetic studies

2.1 Experimental procedures

Transimination with (**DA-X**) as nucleophile

(E)-N-benzyl-1-phenylmethanimine (**BI**) (0.010 mmol, 1.9 µL) was dissolved in 0.50 mL $CDCl_3$. Then the dianiline (**DA-X**) (0.10 mmol, 14.4 mg for **DA-C** or 14.6 mg for **DA-I**) was added to the solution at room temperature. The mixture was briefly shaken and the conversion of **BI** to **IA-X** (Scheme 2A, main text) was followed over time using ^{1}H NMR by integration of the imine signals of the corresponding materials. The imine signal of **BI-I** was typically observed around 8.40 ppm, the imine signal of **IA-C** was typically observed at 8.25 ppm, and the imine signal of **IA-O** was typically observed around 8.29 ppm.

Transimination with **DI-X** as electrophile

Diimine (**DI-X**) (0.010 mmol, 3.20 mg for **DI-C** or 3.24 mg for **DI-O**) was dissolved in 0.50 mL $CDCl_3$. Then benzylamine (**BA**) (0.40 mmol, 44 µL) was added to the solution at room temperature. The mixture was briefly shaken and the conversion of **DI-X** to **BI** (Scheme 2B, main text) was followed over time using ^{1}H NMR by integration of the imine signals of the corresponding materials. The imine signal of **DI-C** was typically observed at 8.28 ppm, and the imine signal of **BI** was typically observed at 8.40-8.41 ppm. The imine signal of **DI-O** was typically observed around 8.26 ppm when both ends were imines, and around 8.30 ppm when one end remained an imine and the other was already transformed back to amine.

Imine metathesis with **DI-X** as nucleophile

(E)-N-benzyl-1-(p-tolyl)methanimine (**TI**) (0.010 mmol, 2.2 µL) was dissolved in 0.50 mL $CDCl_3$. Then the diimine (**DI-X**) (0.20 mmol, 64.1 mg for **DI-C** or 64.9 mg for **DI-O**) was added to the solution at room temperature. The mixture was briefly shaken and the conversion of **TI** to **BI** (Scheme 2C, main text) was followed over time using ^{1}H NMR by integration of the imine signals of the corresponding materials. The imine signal of **TI** was typically observed around 8.37 ppm and the **BI** imine signal was typically observed around 8.41 ppm.

Imine metathesis with **DI-X** as electrophile

Diimine (**DI-X**) (0.010 mmol, 3.20 mg for **DI-C** or 3.24 mg for **DI-O**) was dissolved in 0.50 mL $CDCl_3$. Then **TI** (0.20 mmol, 43 µL) was added at room temperature. The mixture was briefly shaken and the conversion from **DI-X** to **tol$_2$-DI-X** (Scheme 2D, main text) was followed over time using ^{1}H NMR by integration of the imine signals of the corresponding materials. The imine signal of **DI-X** was typically observed around 8.31 ppm, and the imine signal of **tol$_2$-DI-X** was typically observed around 8.27-8.28 ppm. The intermediate **tol-DI-X** (one benzene and one toluene imine) would therefore show one signal at 8.31 ppm and one at 8.27-8.28 ppm. This was included in the integration of the imine signals from benzene-imine to toluene-imine.

2.2 Plots and spectra of the conversion over time

The individual kinetic plots of the conversion over time of the four described exchange reactions are presented in Figures S1–S4. Due to addition of the excess of nucleophilic reactant, a pseudo-first order reaction could be assumed. The data was therefore fitted with the model for first-order kinetics to derive the rate constant k in min^{-1}, which was later converted into 10^3 s^{-1} for better comparison (Table 1, main article text). Stacked ^1H NMR spectra zoomed in on the imine signals are presented in Figure S5–S12 for each individual reaction.

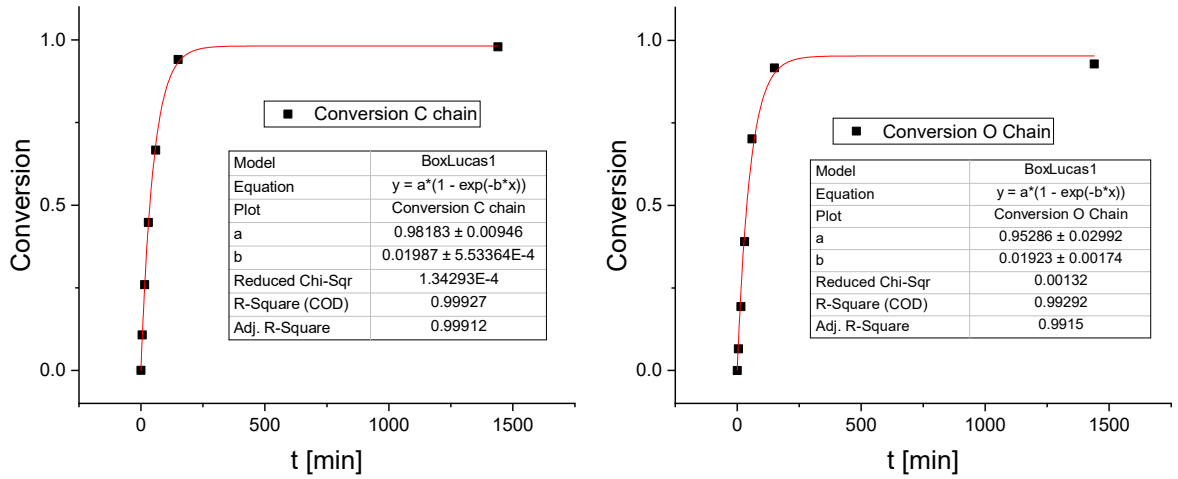

*Figure S1 Kinetic plots of the transimination reaction, for which **DA-C** (left) and **DA-O** (right) acted as nucleophile.*

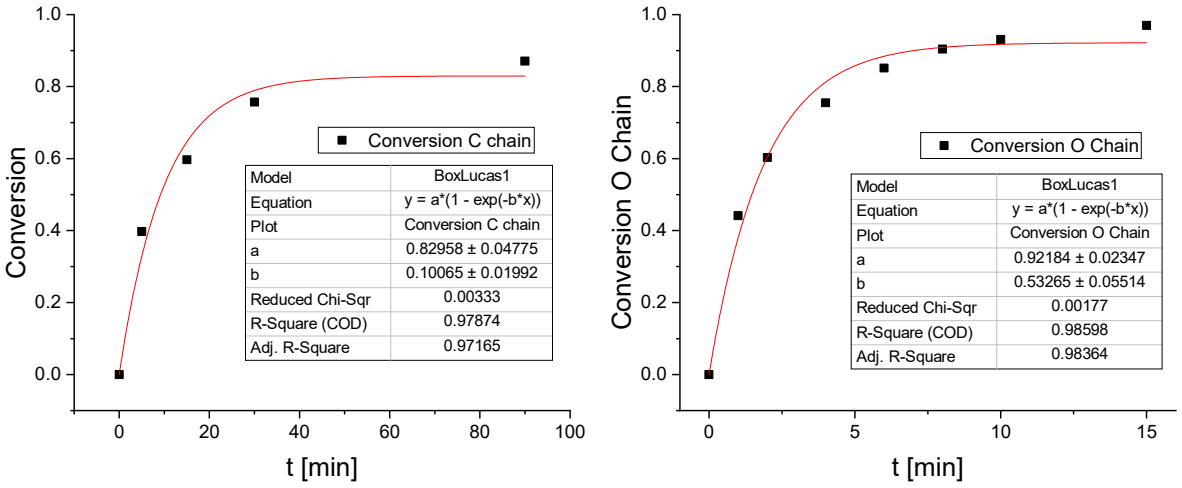

*Figure S2 Kinetic plots of the transimination reaction for which **DI-C** (left) and **DI-O** (right) acted as electrophile.*

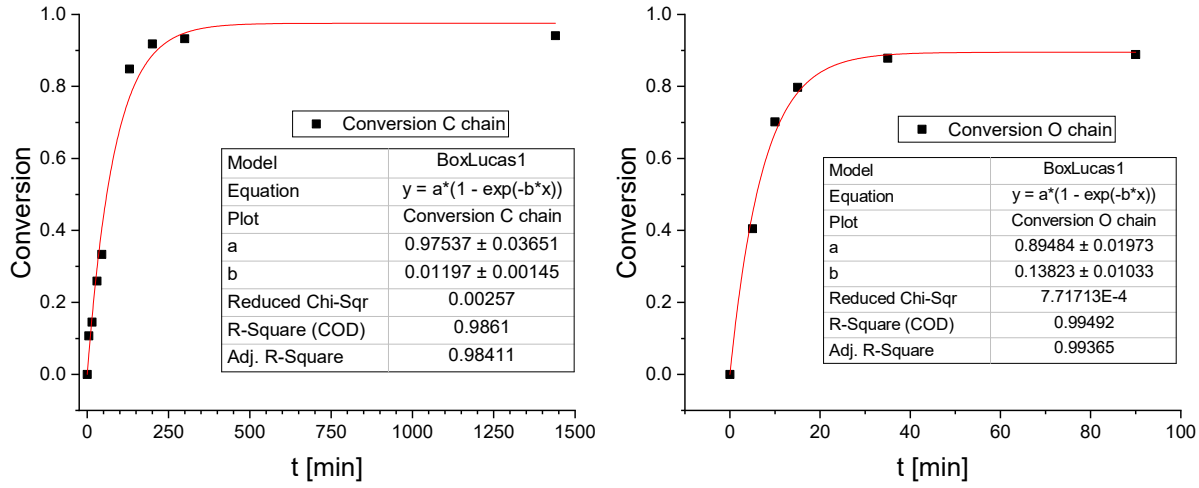

*Figure S3 Kinetic plots of the imine metathesis reaction for which **DI-C** (left) and **DI-O** (right) acted as nucleophile.*

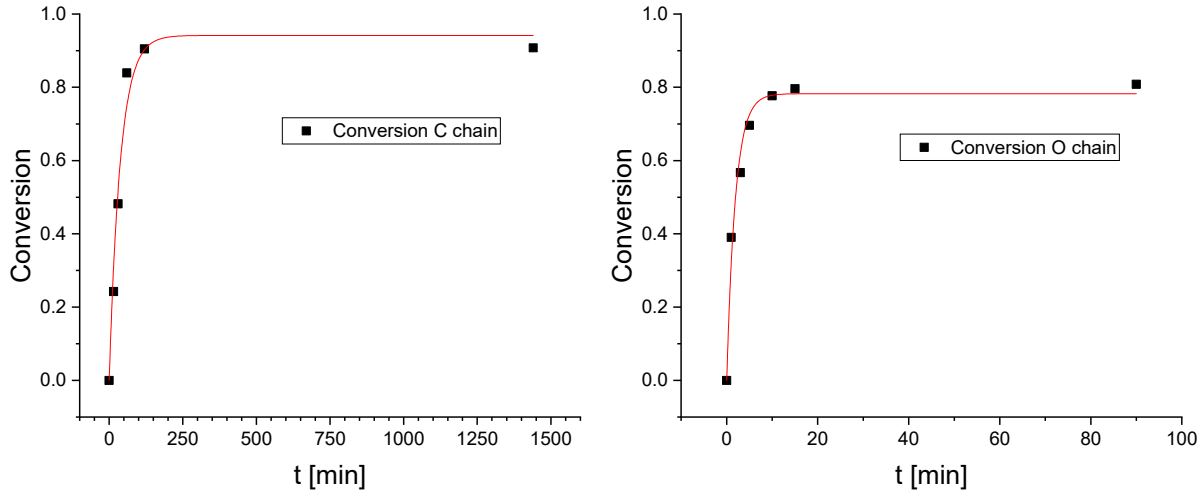

*Figure S4 Kinetic plots of the imine metathesis reaction for which **DI-C** (left) and **DI-O** (right) acted as electrophile.*

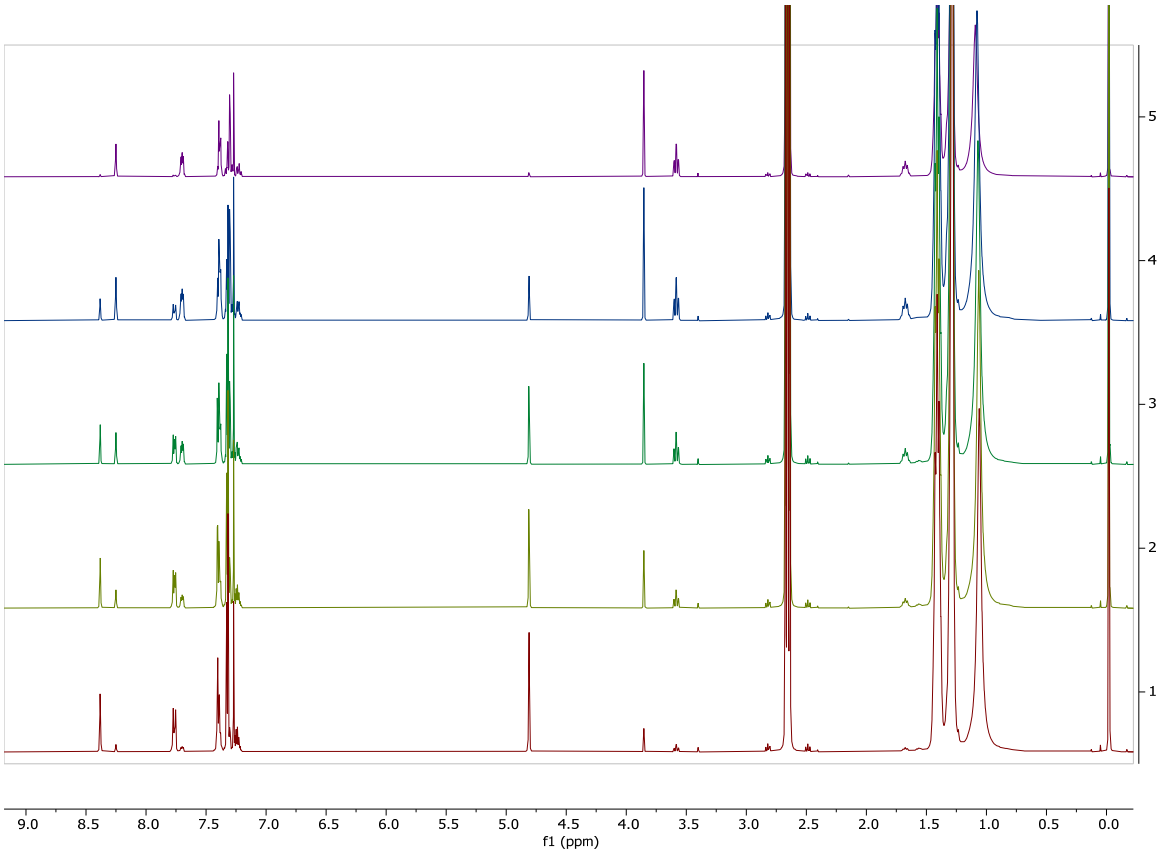

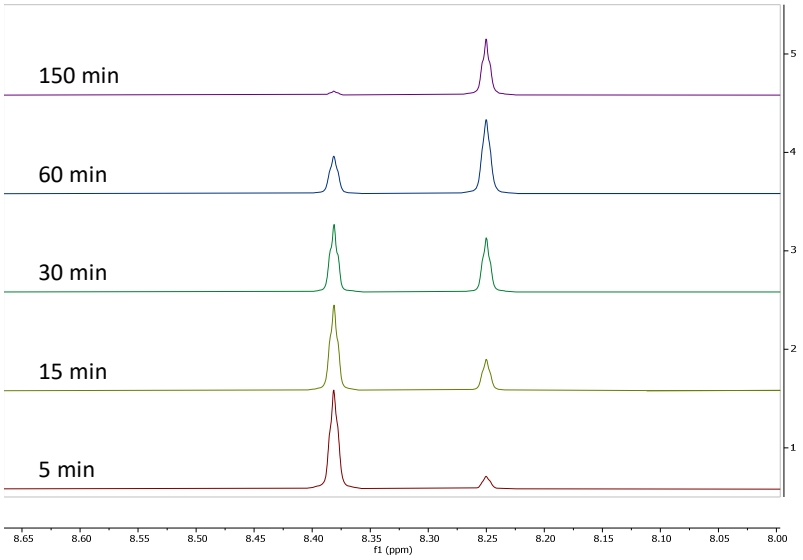

*Figure S5 Top: Representative, stacked ^{1}H NMR spectra of the transimination reaction with **DA-C** as nucleophile at 1) 5 min, 2) 15 min, 3) 30 min, 4) 60 min, 5) 150 min; Bottom: zoomed in spectra of the imine region (8.00-8.65 ppm).*

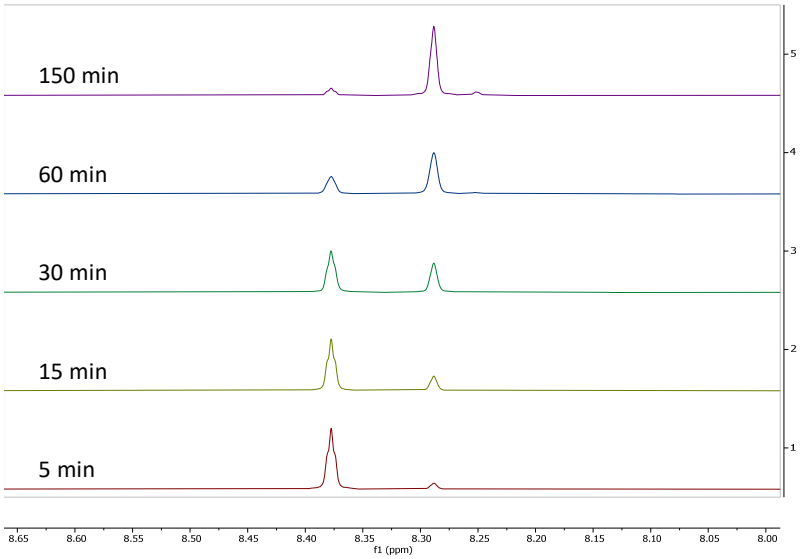

*Figure S6 Stacked ^{1}H NMR spectra of the transimination reaction with **DA-O** as nucleophile, zooming in on the imine region.*

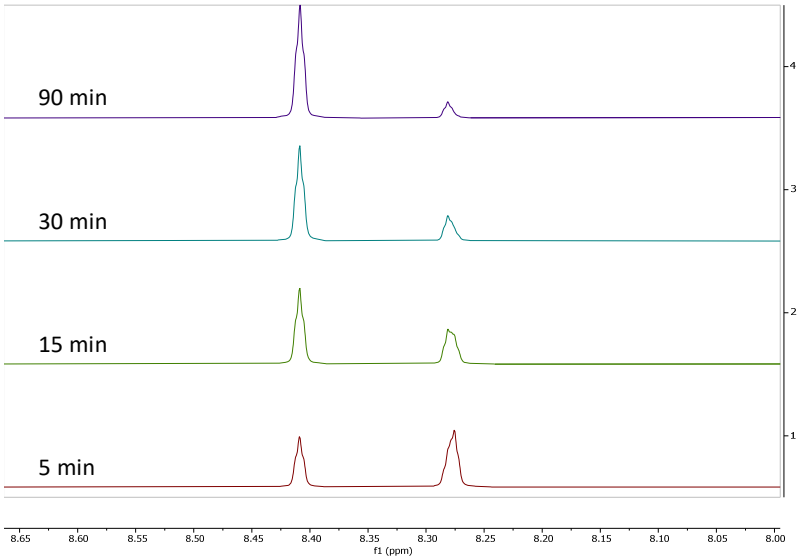

*Figure S7 Stacked ^{1}H NMR spectra of the transimination reaction with **DI-C** as electrophile, zooming in on the imine region.*

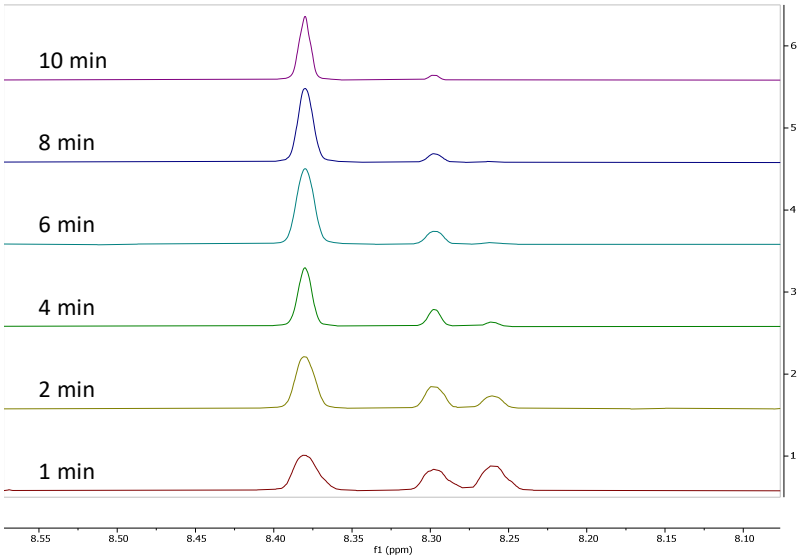

*Figure S8 Stacked [1]H NMR spectra of the transimination reaction with **DI-O** as electrophile, zooming in on the imine region.*

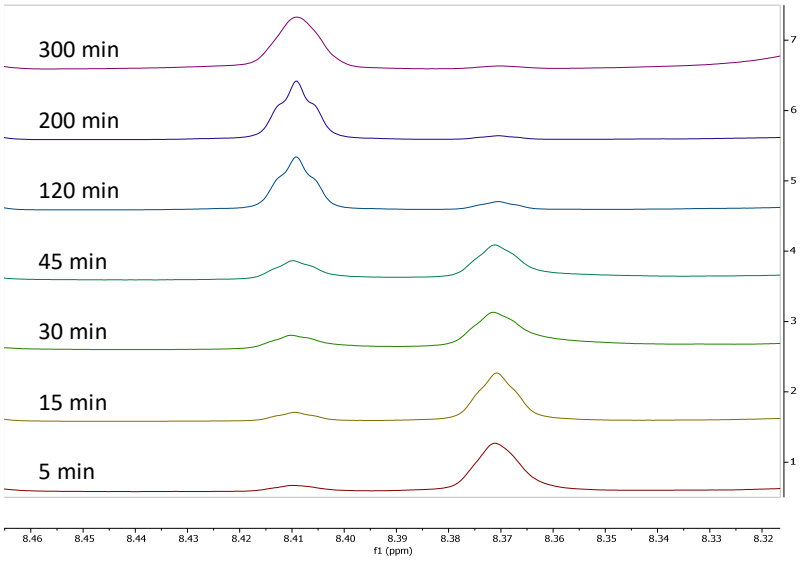

*Figure S9 Stacked [1]H NMR spectra of the metathesis reaction with **DI-C** as nucleophile, zooming in on the imine region.*

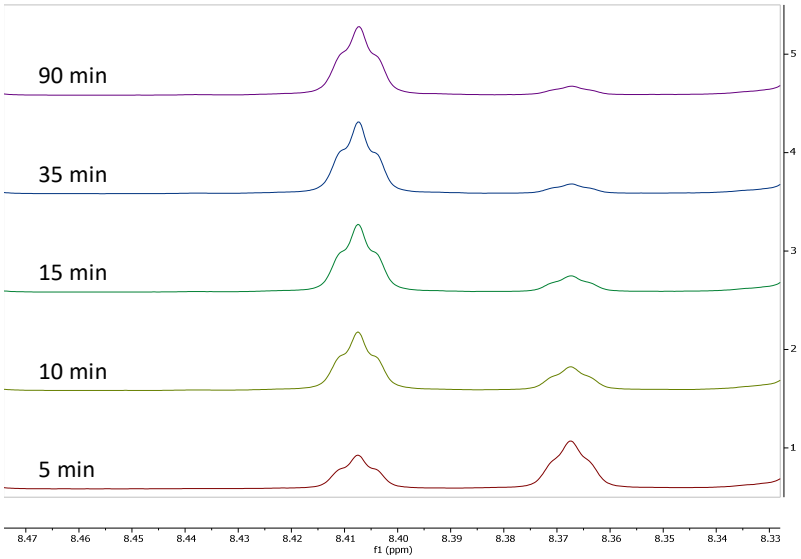

*Figure S10 Stacked ^{1}H NMR spectra of the metathesis reaction with **DI-O** as nucleophile, zooming in on the imine region.*

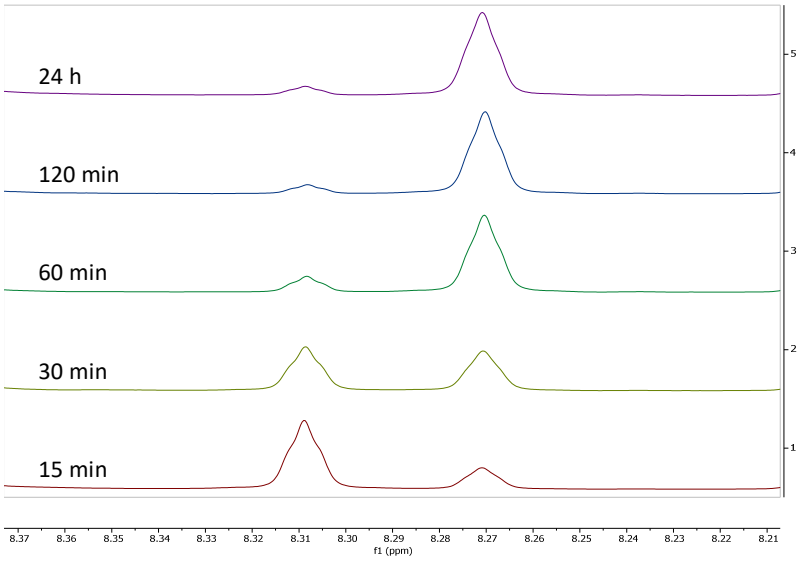

*Figure S11 Stacked ^{1}H NMR spectra of the metathesis reaction with **DI-C** as electrophile, zooming in on the imine region.*

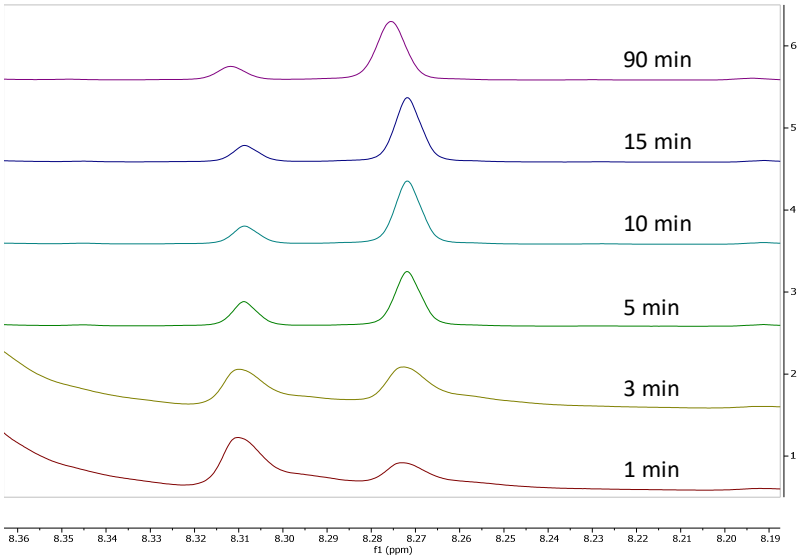

*Figure S12 Stacked ^{1}H NMR spectra of the metathesis reaction with **DI-O** as electrophile, zooming in on the imine region.*

3. Temperature sweep curves of PI-XX materials

All temperature sweep experiments were measured on polymer discs with a 10 mm diameter and 0.40 mm thickness. A constant strain of 0.1% with a frequency of 1 Hz was introduced while gradually heating the sample with 1 °C per 10 s. Storage (*G'*) and loss (*G''*) moduli were plotted as a function of the temperature. The temperature sweep curves for **PI-C** and **PI-O** are presented in Figure 3 in the main article text, and the curves for the **PI-XX** materials are presented in Figure S13 below.

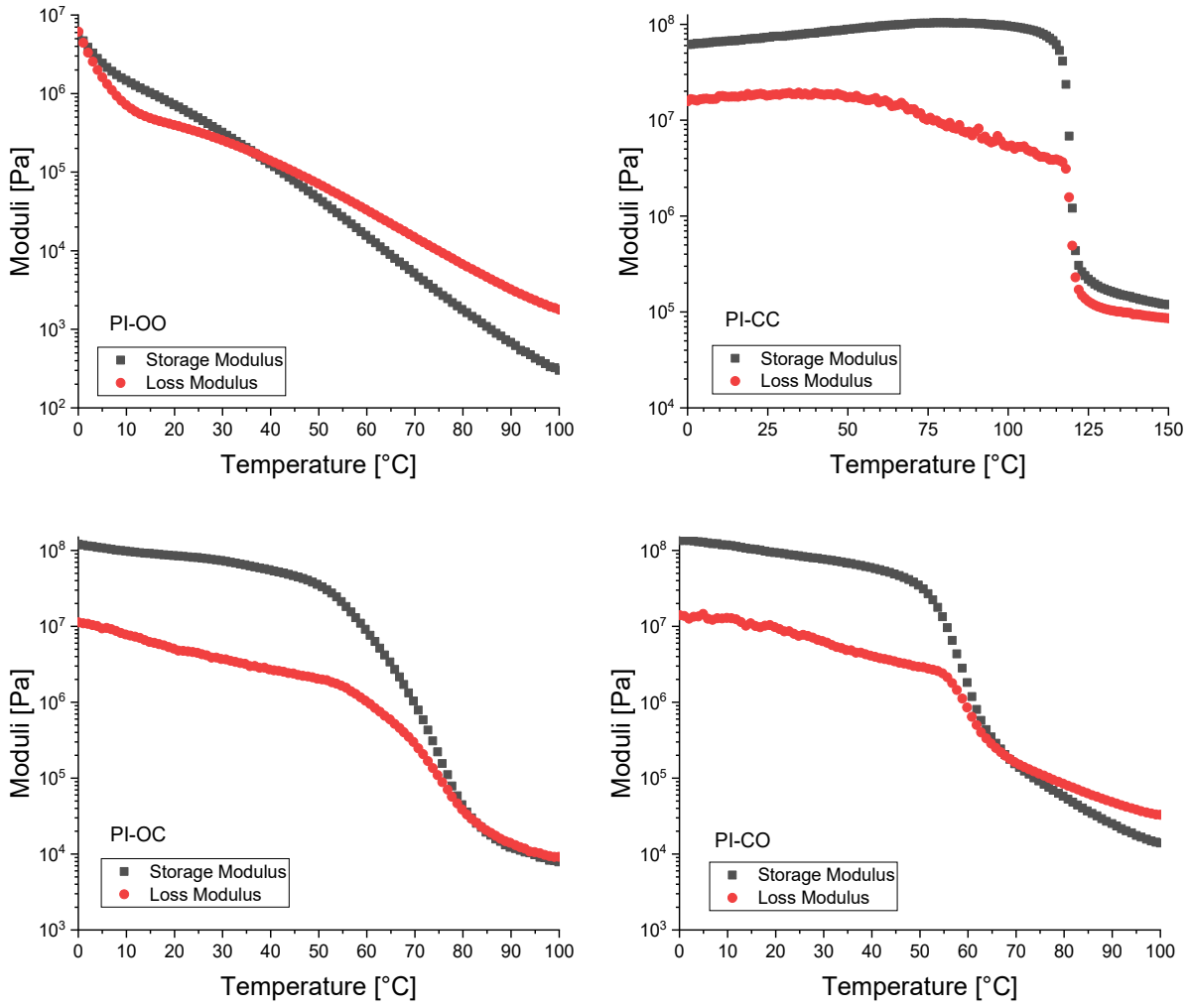

*Figure S13 Temperature sweep curves of **PI-OO** (top left), **PI-CC** (top right), **PI-OC** (bottom left), and **PI-CO** (bottom right).*

4. Stress relaxation

Stress relaxation experiments were performed on polymer discs with a 0.40 mm thickness and 10 mm diameter. The samples were exposed to a 1% strain and the relaxation modulus ($G(t)$) was measured as a function of the time at several temperatures within the rubbery domain of the material. The data was visualised by plotting the relaxation modulus as a function of the time. Following Maxwell's model for stress relaxation the data of the relaxation curves were fitted with a 3-component function of exponential decay:

$$G(t) = A_1 * \exp\left(\frac{-t}{\tau_1}\right) + A_2 * \exp\left(\frac{-t}{\tau_2}\right) + A_3 * \exp\left(\frac{-t}{\tau_3}\right) \quad \text{(eq. S1)}$$

where the first, second and third components represent the network relaxation, imine exchange on local level, and the imine exchange through diffusion, respectively. The determined relaxation times (τ) were tabulated per material at every selected temperature for each of the three relaxation processes (Table S1-S3). The relaxation curves for **PI-O**, **PI-O** and **PI-OO** are shown in Figure S14.

*Table S1 Relaxation times in μs for the three relaxation phases of **PI-O** determined at several temperatures within the rubber region of the material.*

***T* (°C)**	**τ_1 (ms)**	**τ_2 (ms)**	**τ_3 (ms)**
20	13.7 ± 0.4	(4.4 ± 0.3) × 10^2	(184 ± 9) × 10^2
25	13.2 ± 0.5	(3.3 ± 0.2) × 10^2	(96 ± 3) × 10^2
30	12.1 ± 0.6	(2.3 ± 0.2) × 10^2	(51 ± 1) × 10^2
35	9.0 ± 0.6	(1.4 ± 0.1) × 10^2	(277 ± 7) × 10^1
40	7.3 ± 0.5	(1.0 ± 0.1) × 10^2	(163 ± 3) × 10^1
45	5.5 ± 0.4	(7.4 ± 0.4) × 10^1	(102 ± 1) × 10^1
50	5.0 ± 0.4	(6.3 ± 0.3) × 10^1	(67 ± 1) × 10^1
55	4.1 ± 0.3	(5.6 ± 0.3) × 10^1	(460 ± 7) × 10^0

*Table S2 Relaxation times in μs for the three relaxation phases of **PI-C** determined at several temperatures within the rubber region of the material.*

***T* (°C)**	**τ_1 (ms)**	**τ_2 (ms)**	**τ_3 (ms)**
140	1.0 ± 0.1	112 ± 4	(5 ± 1) × 10^2
145	1.0 ± 0.1	94 ± 4	(4 ± 1) × 10^2
150	1.0 ± 0.1	83 ± 4	(3 ± 1) × 10^2
155	1.0 ± 0.1	77 ± 3	(4 ± 1) × 10^2
160	1.0 ± 0.1	70 ± 3	(4 ± 1) × 10^2
165	1.0 ± 0.1	65 ± 2	(5 ± 2) × 10^2
170	1.1 ± 0.1	59 ± 2	(5 ± 3) × 10^2
175	1.1 ± 0.1	56 ± 2	(5 ± 3) × 10^2

*Table S3 Relaxation times in μs for the three relaxation phases of **PI-OO** determined at several temperatures within the rubber region of the material.*

***T* (°C)**	**τ_1 (ms)**	**τ_2 (ms)**	**τ_3 (ms)**
15	11.0 ± 0.2	(37 ± 3) × 10^1	(12 ± 1) × 10^3
20	10.0 ± 0.4	(27 ± 2) × 10^1	(73 ± 5) × 10^2
25	8.0 ± 0.5	(17 ± 1) × 10^1	(40 ± 2) × 10^2
30	5.7 ± 0.4	(11 ± 1) × 10^1	(22 ± 1) × 10^2
35	4.1 ± 0.4	76 ± 3	(13 ± 1) × 10^2
40	2.7 ± 0.5	58 ± 2	(86 ± 3) × 10^1
45	2.3 ± 0.4	52 ± 2	(64 ± 2) × 10^1
50	1.4 ± 0.1	50 ± 2	(48 ± 2) × 10^1

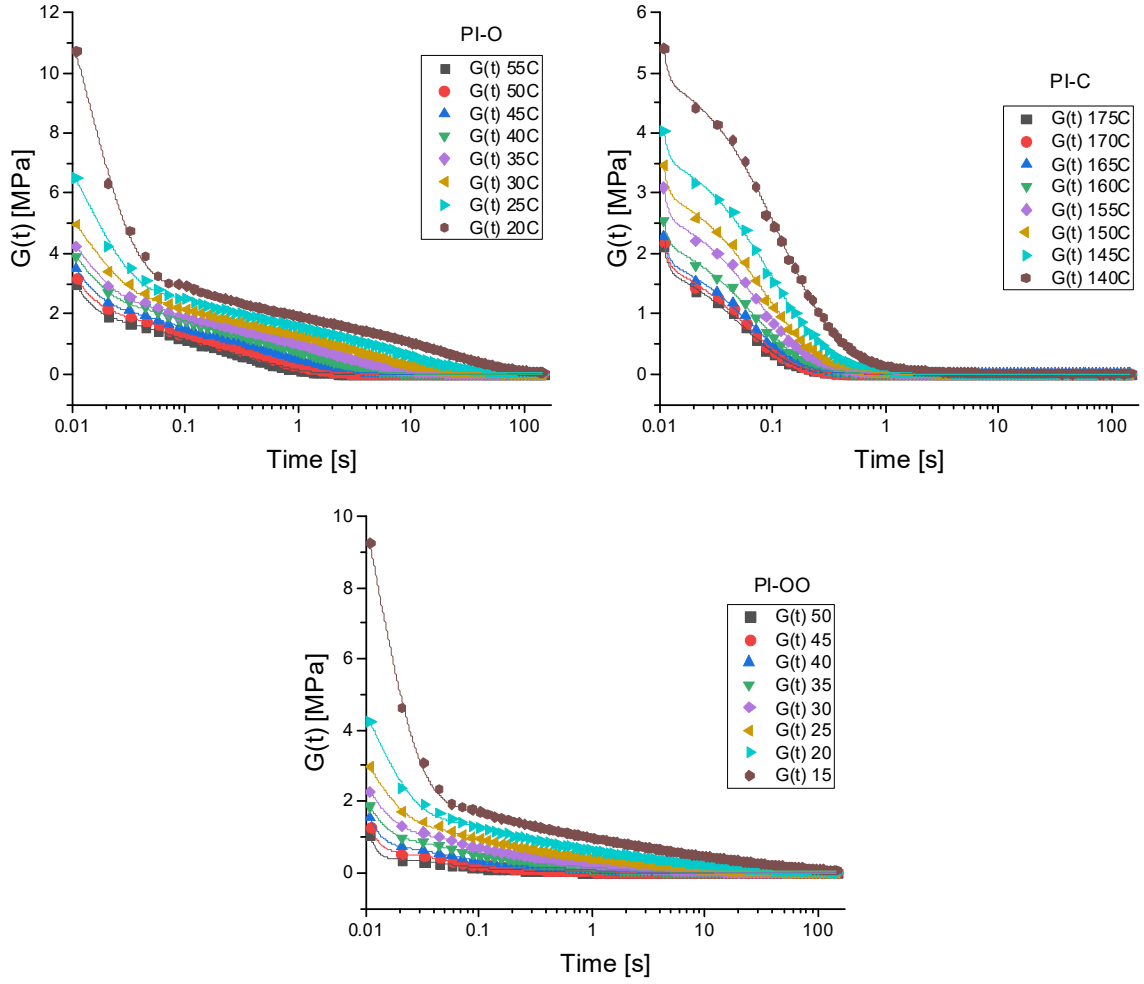

*Figure S14 Stress relaxation curves of **PI-O** (top left), **PI-C** (top right), and **PI-OO** (bottom). Data points were fitted according to a 3-component exponential decay.*

5. Synthetic procedures and analyses

5.1 Synthesis and analysis of small-molecule analogues and monomers

*(E)-N-benzyl-1-phenylmethanimine (**BI**)*

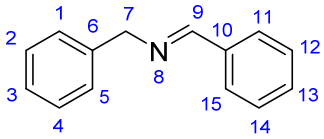

Benzaldehyde (0.52 mL, 5.1 mmol) and benzylamine (0.56 mL, 5.1 mmol) were dissolved in dichloromethane (50 mL). Molecular sieves (3 Å) were added and the mixture was stirred at room temperature for 3 hours. Afterwards, the mixture was filtered over Celite®. The filtrate was concentrated *in vacuo* to obtain the product as a clear yellow liquid with a 99% yield.

R_f: 0.55 (EtOAc/heptane 1:9).

^{1}H NMR (400 MHz, $CDCl_3$, *δ*): 8.41 (s, C9-H, 1H), 7.81-7.78 (m, C11-H + C15-H, 2H), 7.44-7.43 (m, C12-H + C14-H, 2H), 7.42 (m, C13-H, 1H), 7.36-7.35 (m, C1-H + C2-H + C4-H + C5-H, 4H), 7.30-7.25 (m, C3-H, 1H), 4.84 (s, C7-H, 1H).

^{13}C NMR (100 MHz, $CDCl_3$, *δ*): 162.6 (C9), 138.9 (C6), 136.3 (C10), 131.6 (C12 + C14), 128.7 (C13), 128.6 (C2 + C4), 128.4 (C11 + C15), 128.1 (C1 + C5), 126.2 (C3), 65.2 (C7).

*(E)-N-benzyl-1-(p-tolyl)methanimine (**TI**)*

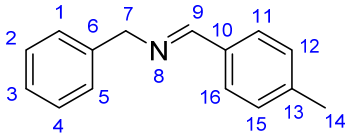

p-Tolualdehyde (0.59 mL, 5.0 mmol) and benzylamine (0.55 mL, 5.0 mmol) were dissolved in dichloromethane (50 mL). Molecular sieves (3 Å) were added and the mixture was stirred at room temperature for 3 hours. Afterwards, the mixture was filtered over Celite®. The filtrate was concentrated *in vacuo* to obtain the product as a colourless liquid with a 98% yield.

R_f: 0.51 (EtOAc/Heptane 1:9).

^{1}H NMR (400 MHz, $CDCl_3$, *δ*): 8.38 (s, C9-H, 1H), 7.70-7.68 (d, *J* = 8.2 Hz, C11-H + C16-H, 2H), 7.36-7.35 (m, C1-H + C2-H + C4-H + C5-H, 4H), 7.30-7.26 (m, C3-H, 1H), 7.25-7.23 (t, *J* = 8.3 Hz, C12-H + C15-H, 2H), 4.83 (s, C7-H, 2H), 2.40 (s, C14-H, 3H).

^{13}C NMR (100 MHz, $CDCl_3$, *δ*): 162.1 (C9), 141.2 (C13), 139.6 (C6), 133.7 (C10), 129.5 (C12 + C15), 128.6 (C2 + C4), 128.4 (C11 + C16), 128.1 (C1 + C5), 127.1 (C3), 65.2 (C7), 21.6 (C14).

*(1E,1'E)-N,N'-(octane-1,8-diyl)bis(1-phenylmethanimine) (**DI-C**)*

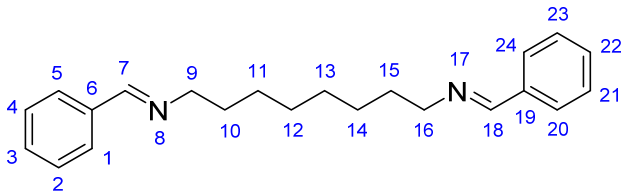

Benzaldehyde (0.63 mL, 6.2 mmol) and 1,8-diaminooctane (0.45 g, 3.1 mmol) were dissolved in dichloromethane (50 mL). Molecular sieves (3 Å) were added and the mixture was stirred at room temperature for 3 hours. Afterwards, the mixture was filtered over Celite®. The filtrate was concentrated *in vacuo* to obtain the product as a white crystalline solid with an 84% yield.

R_f: 0.45 (EtOAc/Heptane 1:9).

^{1}H NMR (400 MHz, $CDCl_3$, *δ*): 8.27 (s, C7-H + C18-H, 2H), 7.73-7.71 (m, C1-H + C5-H + C20-H + C24-H, 4H), 7.41-7.40 (m, C2-H + C3-H + C4-H + C21-H + C22-H + C23-H, 6H), 3.62-3.58 (t, *J* =

7.2 Hz, C9-H + C16-H, 4H), 1.71-1.68 (m, C10-H + C15-H, 4H) 1.36 (m, C11-H + C12-H + C13-H + C14-H, 8H).

^{13}C NMR (100 MHz, $CDCl_3$, δ): 160.9 (C7 + C18), 136.5 (C6 + C19), 130.6 (C3 + C22), 128.7 (C2 + C4 + C21 + C23), 128.2 (C1 + C5 + C20 + C24), 62.0 (C9 + C16), 31.0 (C10 + C15), 29.5 (C12 + C13), 27.5 (C11 + C14).

*(1E,1'E)-N,N'-((ethane-1,2-diylbis(oxy))bis(ethane-2,1-diyl))bis(1-phenylmethanimine) (**DI-O**)*

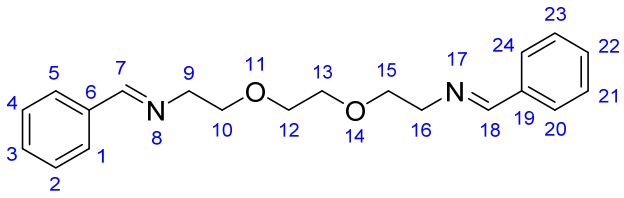

Benzaldehyde (0.63 mL, 6.2 mmol) and 1,2-bis(2-aminoethoxy)ethane (0.45 mL, 3.1 mmol) were dissolved in dichloromethane (50 mL). Molecular sieves (3 Å) were added and the mixture was stirred at room temperature for 3 hours. Afterwards, the mixture was filtered over Celite®. The filtrate was concentrated *in vacuo* to obtain the product as a colourless oil with an 82% yield.

R_f: 0.45 (EtOAc/Heptane 1:9).

^{1}H NMR (400 MHz, $CDCl_3$, δ): 8.28 (s, C7-H + C18-H, 2H), 7.73-7.71 (m, C1-H + C5-H + C20-H + C24-H, 4H), 7.41-7.39 (m, C2-H + C3-H + C4-H + C21-H + C22-H + C23-H, 6H), 3.77 (s, C10-H + C12-H + C13-H + C15-H, 8H), 3.63 (s, C9-H + C16-H, 4H).

^{13}C NMR (400 MHz, $CDCl_3$, δ): 162.8 (C7 + C18), 136.3 (C6 + C19), 130.8 (C2 + C4 + C21 + C23), 128.7 (C3 + C22), 128.3 (C1 + C5 + C20 + C24), 70.9 (C10 + C15), 70.7 (C12 + C13), 61.3 (C9 + C16).

*4,4'-(octane-1,8-diylbis(oxy))dibenzaldehyde (**AL-C**)*

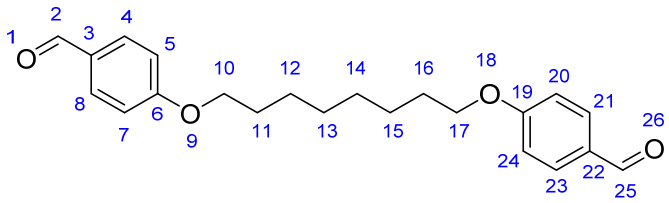

4-Hydroxybenzaldehyde (2.44 g, 20.0 mmol) was dissolved in EtOH (25 mL). A solution of NaOH (863 mg, 21.6 mmol) in water (10 mL) was slowly added and the mixture stirred for 15 min at room temperature. 1,8-Dibromooctane (1.88 mL, 10.0 mmol) was added to the reaction mixture, which was then heated to reflux for overnight. The mixture was slowly cooled to room temperature and then placed on an ice bath so that a white solid precipitated from the solution. The solid was captured by filtration and rinsed with cold water. It was then dried *in vacuo* to obtain the product as a white powder with an 83% yield.

R_f: 0.56 (EtOAc/heptane 1:1)

^{1}H NMR (400 MHz, $CDCl_3$, δ): 9.88 (s, C2-H + C25-H, 2H), 7.84-7.81 (d, J = 8.75 Hz, C4-H + C8-H + C21-H + C23-H + 4H), 7.00-6.98 (d, J = 8.72, C5-H + C7-H + C20-H + C24-H, 4H), 4.06-4.03 (t, J = 6.47, C10-H + C17-H, 4H), 1.86-1.79 (m, C11-H + C16-H, 4H), 1.53-1.48 (m, C12-H + C15-H, 4H), 1.43-1.39 (m, C13-H + C14-H, 4H).

^{13}C NMR (100 MHz, $CDCl_3$, δ): 190.9 (C2 + C25), 164.4 (C6 + C19) 132.1 (C4 + C8 + C21 + C23), 129.9 (C3 + C22), 114.9 (C5 + C7 + C20 + C24), 68.5 (C10 + C17), 29.4 (C12 + C15), 29.2 (C11 + C16), 26.0 (C13 + C14).

*4,4'-(((ethane-1,2-diylbis(oxy))bis(ethane-2,1-diyl))bis(oxy))dibenzaldehyde (**AL-O**)*

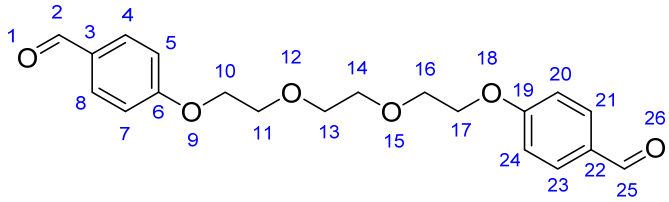

4-Hydroxybenzaldehyde (6.69 g, 54.8 mmol) was dissolved in DMF (100 mL). NaOH (2.67 g, 66.8 mmol) was slowly added to the solution, which then stirred for 15 min at room temperature. Triglycol dichloride (4.28 mL, 27.4 mmol) was slowly added to the reaction mixture, which was then heated to reflux for overnight. The reaction mixture was cooled to room temperature before pouring onto ice chunks. A white precipitate formed, which was captured by filtration and rinsed with cold water. The wet material was dried *in vacuo* to obtain the product as a beige powder with a 28% yield.

R_f: 0.41 (EtOAc/heptane 1:1).

^{1}H NMR (400 MHz, $CDCl_3$, *δ*): 9.87 (s, C2-H + C25-H, 2H), 7.81 (d, *J*=8.8 Hz, C4-H + C8-H + C21-H + C23-H, 4H), 7.00 (d, *J*=8.7 Hz, C5-H + C7-H + C20-H + C24-H, 4H), 4.20 (t, *J* = 4.8 Hz, C10-H + C17-H, 4H), 3.89 (t, *J*=4.8 Hz, C11-H + C16-H, 4H), 3.76 (s, C13-H + C14-H, 4H).

^{13}C NMR (100 MHz, $CDCl_3$, *δ*): 190.9 (C2 + C25), 163.9 (C6 + C19), 132.1 (C4 + C8 + C21 + C23), 130.2 (C3 + C22), 115.0 (C5 + C7 + C20 + C24), 71.1 (C13 + C14), 69.7 (C11 + C16) 67.9 (C10 + C17)

5.2 General procedure for polymer synthesis[S1]

Tris(2-aminoethyl)amine (30 µL, 0.20 mmol) and diamine (**DA-C**: 534 mg, 3.70 mmol *or* **DA-O**: 540 µL, 3.70 mmol) were dissolved in 5 mL THF. Then the dialdehyde (**TA**: 537 mg, 4.00 mmol *or* **AL-C**: 1.42 g, 4.00 mmol *or* **AL-O**: 1.43 g, 4.00 mmol) was added, and the mixture was shaken until a homogeneous solution was obtained. The solution was poured into a petri dish and left for overnight. To remove remaining solvent and formed water from the polymers, they were further dried in a vacuum oven at 50 °C for another day. FT-IR was used to check full conversion of the aldehydes (1700 cm^{-1}) to imine (1640 cm^{-1}). The FT-IR spectra of all polymer materials are shown in Figure S15. In order to further analyse the materials with rheology, they were hot-pressed (max. 40 N and 150 °C, depending on the material) into discs with a 10 mm diameter and 0.4 mm thickness.

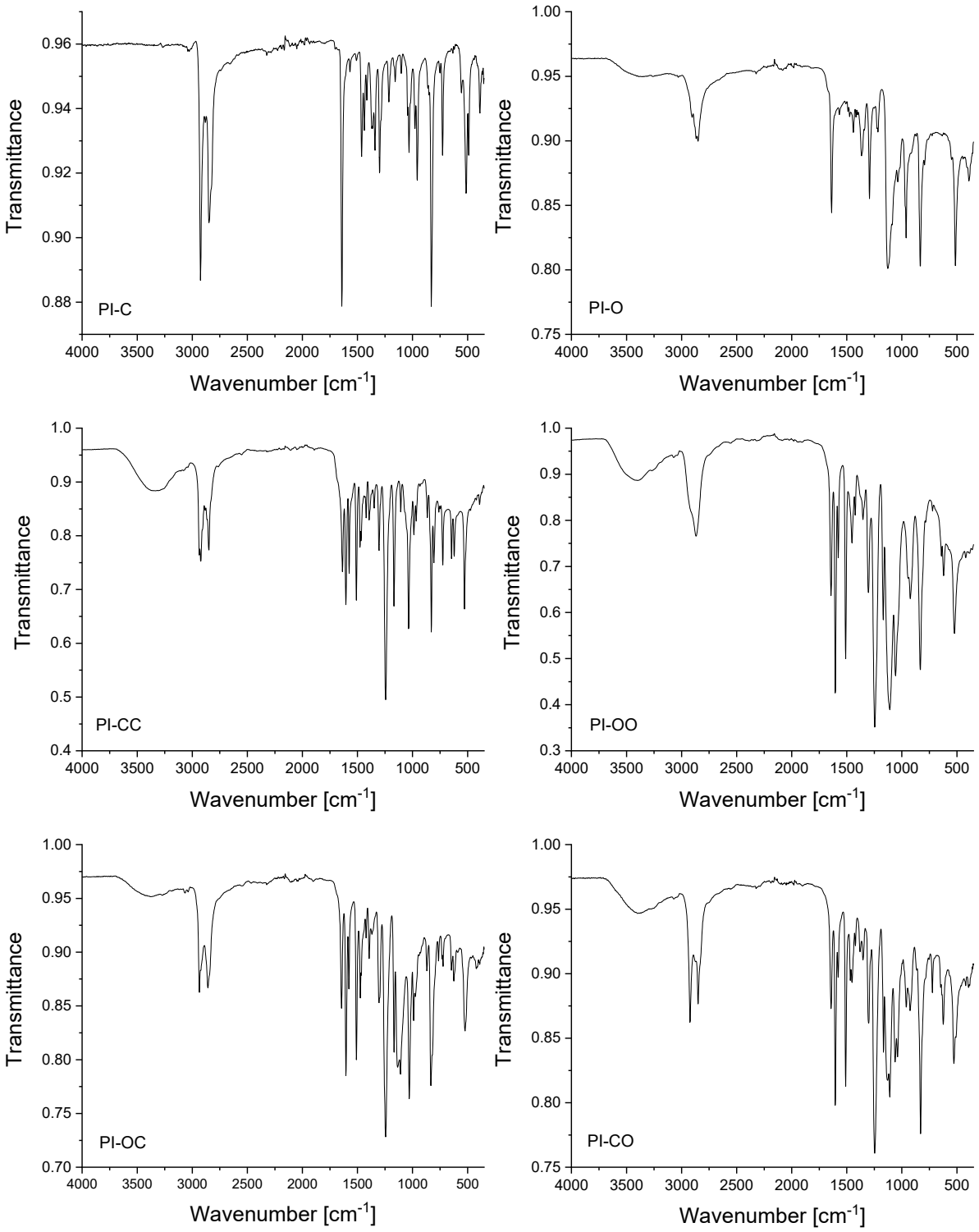

*Figure S15 FT-IR spectra of **PI-C** (top left), **PI-O** (top right), **PI-CC** (middle left), **PI-OO** (middle right), **PI-OC** (bottom left), and **PI-CO** (bottom right). Disappearance of the aldehyde signal (1700 cm^{-1}) and appearance of the imine signal (1640 cm^{-1}) was used to confirm formation of the polyimines.*

6. Supporting NMR spectra

^{1}H NMR and ^{13}C NMR spectra of BI

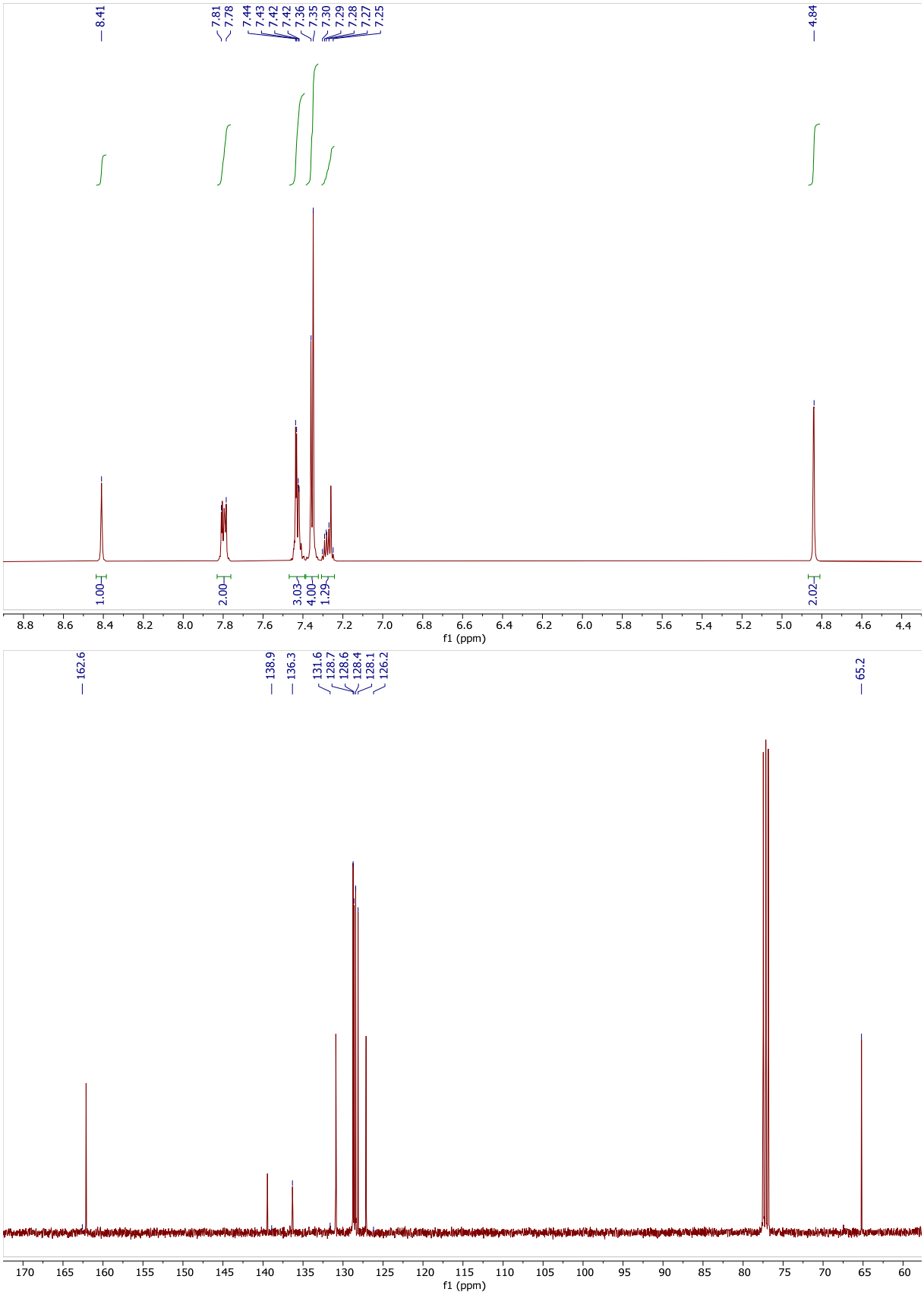

*Figure S16 ^{1}H (top) and ^{13}C (bottom) NMR spectrum of **BI**, recorded at 298 K in $CDCl_3$.*

^{1}H NMR and ^{13}C NMR spectra of TI

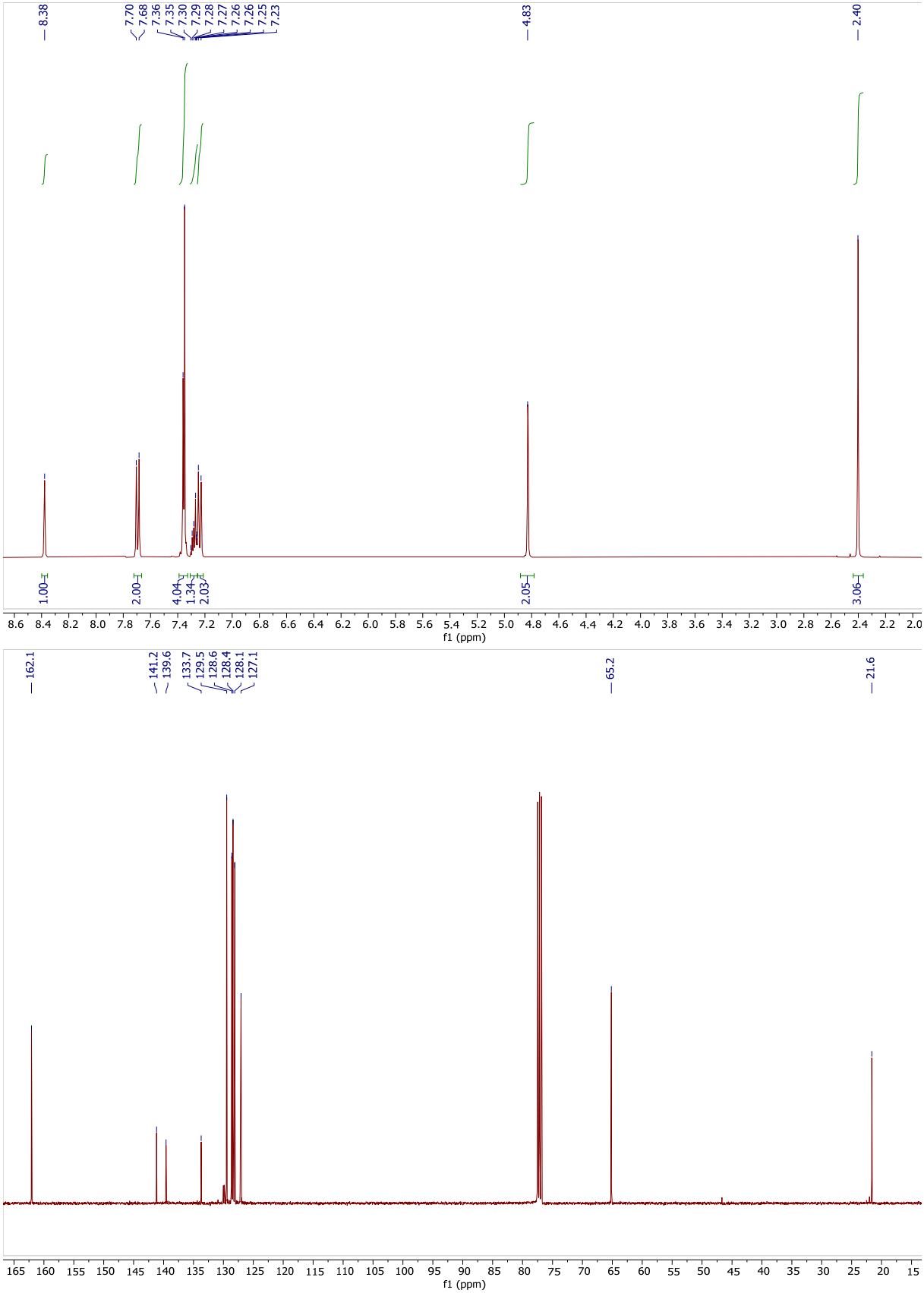

*Figure S17 ^{1}H (top) and ^{13}C (bottom) NMR spectrum of **TI**, recorded at 298 K in $CDCl_3$.*

^{1}H NMR and ^{13}C NMR spectra of DI-C

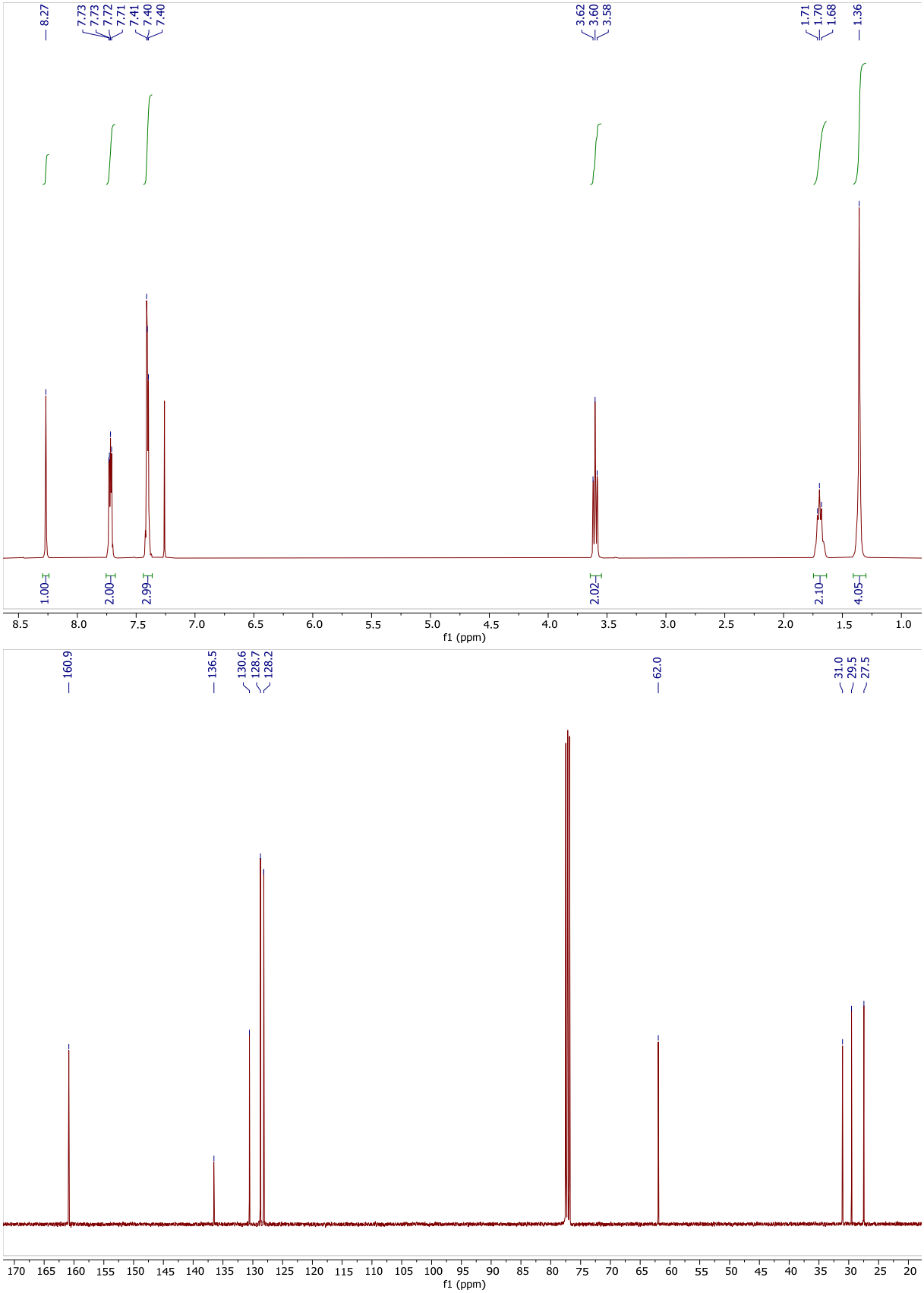

*Figure S18 ^{1}H (top) and ^{13}C (bottom) NMR spectrum of **DI-C**, recorded at 298 K in $CDCl_3$.*

^{1}H NMR and ^{13}C NMR spectra of DI-O

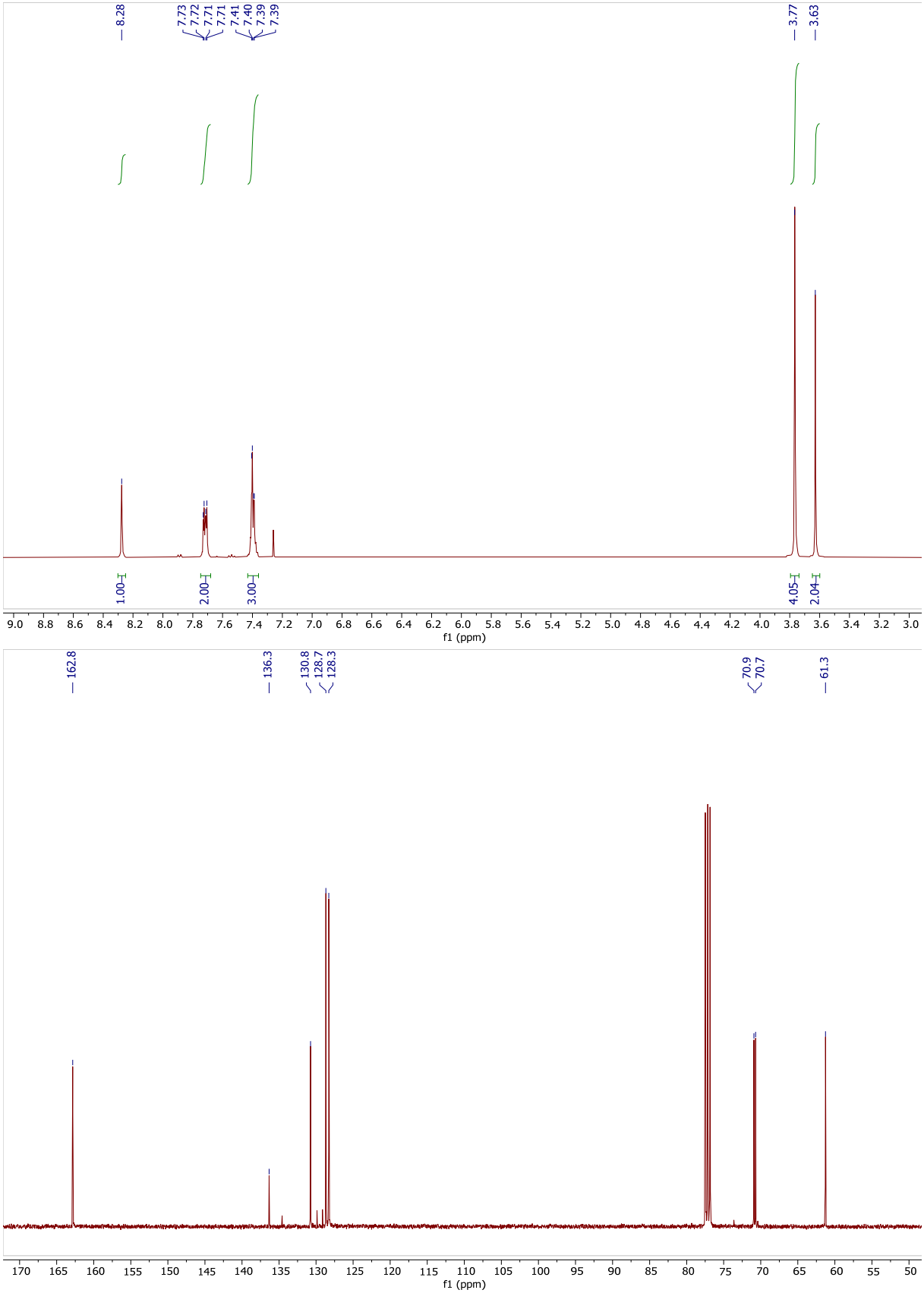

*Figure S19 ^{1}H (top) and ^{13}C (bottom) NMR spectrum of **DI-O**, recorded at 298 K in $CDCl_3$.*

^{1}H NMR and ^{13}C NMR spectra of AL-C

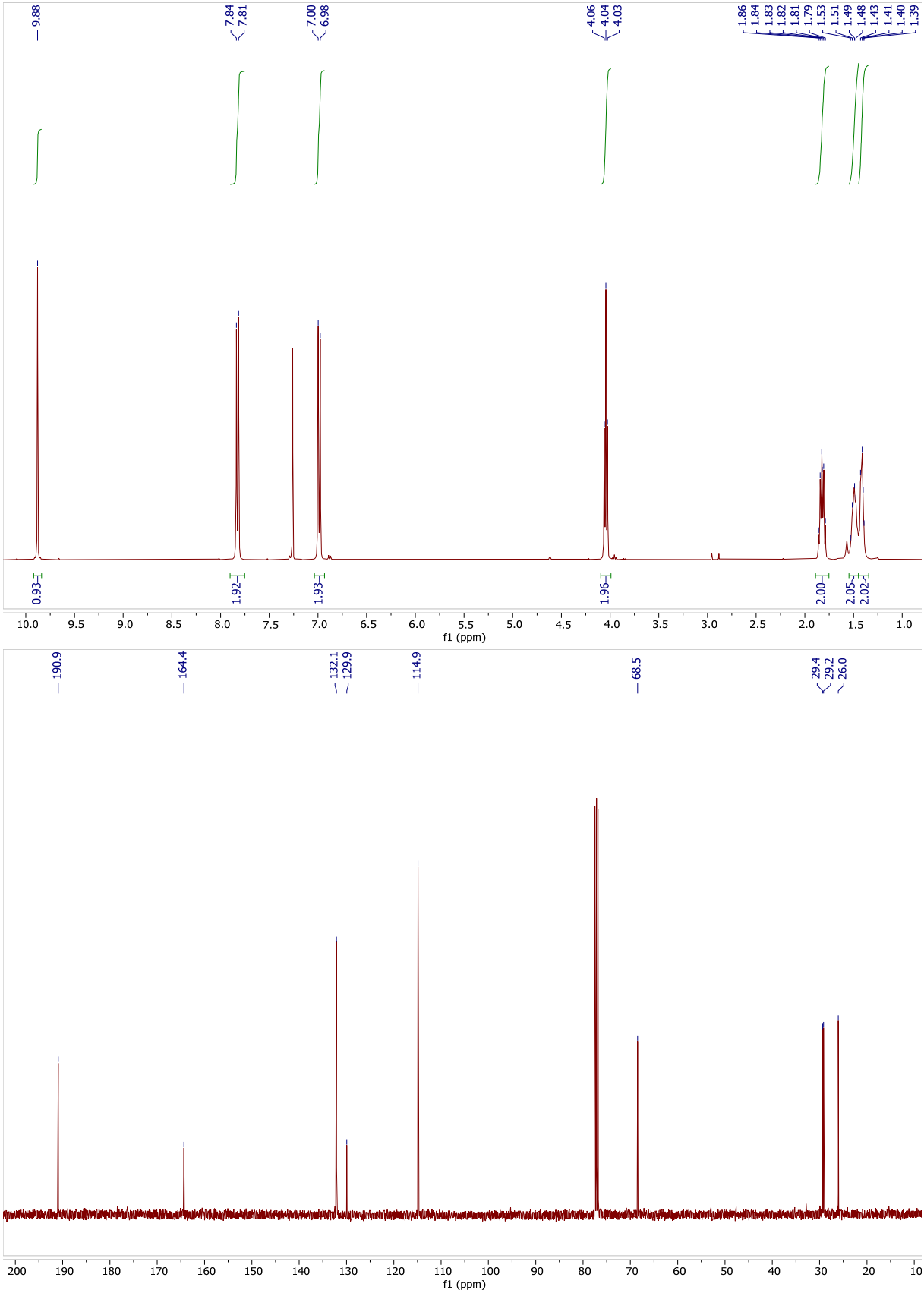

*Figure S20 ^{1}H (top) and ^{13}C (bottom) NMR spectrum of **AL-C**, recorded at 298 K in $CDCl_3$.*

^{1}H NMR and ^{13}C NMR spectra of AL-O

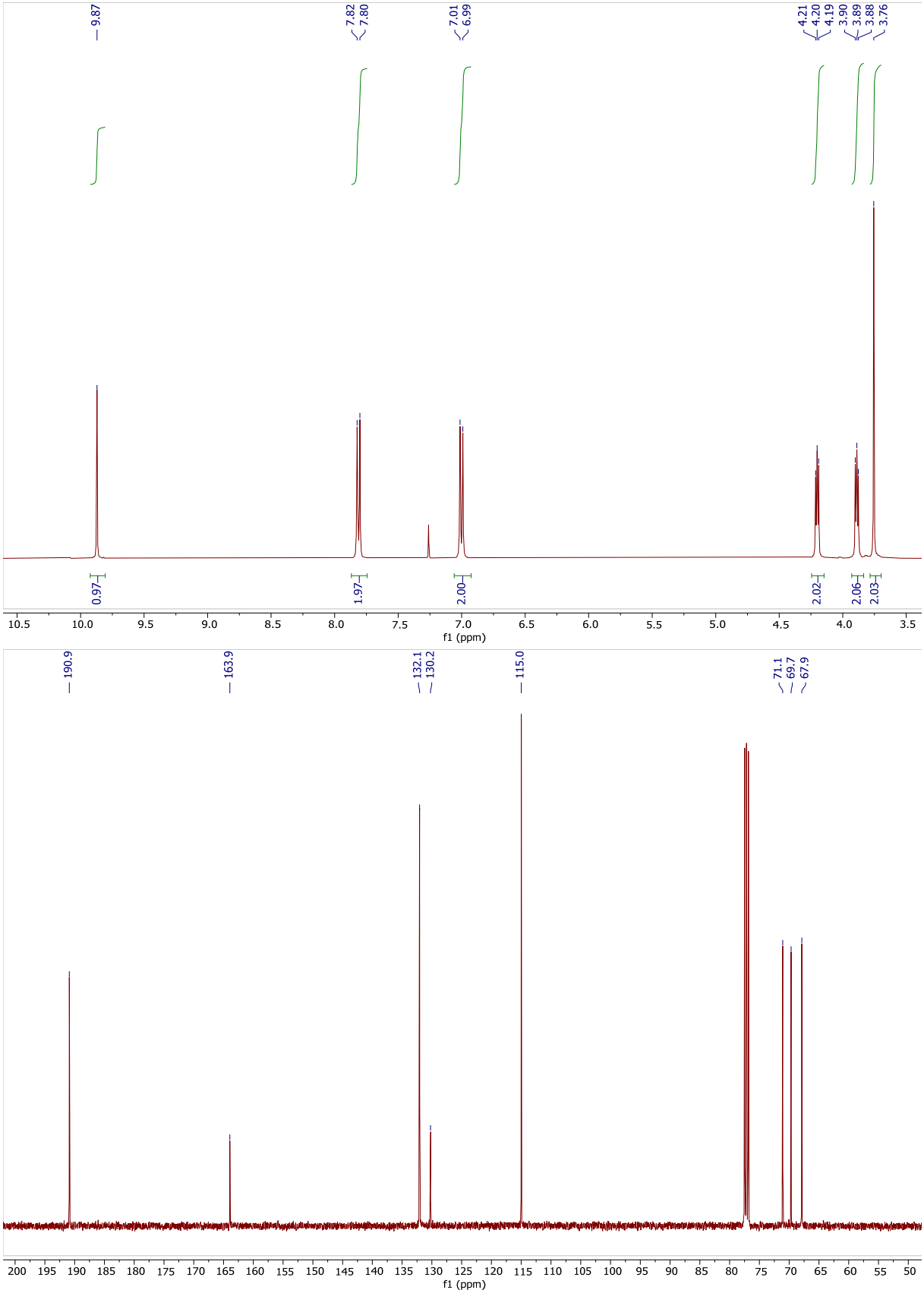

*Figure S21 ^{1}H (top) and ^{13}C (bottom) NMR spectrum of **AL-O**, recorded at 298 K in $CDCl_3$.*

7. References

S1. S. K. Schoustra, J. Dijksman, H. Zuilhof and M. M. J. Smulders, *Chem. Sci.*, 2020, **Advance Article**, DOI:10.1039/D1030SC05458E